Research Square

Preprints are preliminary reports that have not undergone peer review.
They should not be considered conclusive, used to inform clinical practice,
or referenced by the media as validated information.

Polarization Stability and Nanoscale Ferroelectric Switching in Self- Assembled PVDF Nanodots on Glass Substrate After Poling

Shalini Selvam
Saveetha Institute of Medical And Technical Sciences
Suganthi Muthusamy
St. Joseph's Institute of Technology, OMR, Chennai
M Perumal
AMET University, Kanathur, Chennai
Suvitha A
S.A Engineering College (An Autonomous Institution), Chennai 600077
M S Ravisankar
ravisankarms775@gmail.com
Saveetha Institute of Medical And Technical Sciences
V. Balasubramani
Saveetha Institute of Medical And Technical Sciences
J Venkatamuthukumar
Raja Lakshmi Engineering College, Thandalam

Research Article

Keywords: Nanodots, Relaxation Kinetics, Stretched exponential function, Natural ferroelectric shape memory devices, Flexible electronics

Posted Date: April 10th, 2026

DOI: https://doi.org/10.21203/rs.3.rs-9132602/v1

License: This work is licensed under a Creative Commons Attribution 4.0 International License.
Read Full License

Additional Declarations: No competing interests reported.

Version of Record: A version of this preprint was published at Journal of Nanoparticle Research on June 25th, 2026. See the published version at https://doi.org/10.1007/s11051-026-06694-y.

Abstract

The relaxation behavior of self-assembled polyvinylidene fluoride (PVDF) nanodots on glass substrate with 220 nm thickness, after electrical poling was systematically investigated using piezo response force microscopy (PFM). Time progression of − 10 V (UP) and + 10 V (DOWN) polarized domains of PVDF film kept at room temperature revealed destabilization of already-established polarized ferroelectric domains. Following the PVDF films poled UP and DOWN, the self-polarization effect first produces a uniform UP polarization. UP-polarized domains start to form during the next 2.30 hours of relaxation, which reflects a slow shift in the material's vertical response. Electrical poling under ± 10 biases induced a clear 180° phase contrast, confirming reversible ferroelectric polarization switching, coercive voltages − 0.5 V to 2.3 V and strong piezoelectric coupling with a maximum local d_{33} value of ~ 6.65 nm/V. Furthermore, information from hysteresis loops, butterfly curves, and surface potential measurements show that the migration of mobile space charges is a major factor in speeding up this relaxation process. The temporal evolution of polarization was well described by a stretched exponential model, revealing excellent stability. These findings, analogous to electric stimulate shape-memory systems, highlighting their potential for advanced ferroelectric and flexible electronic applications.

Highlights

- Highly ordered PVDF nanodot arrays were fabricated via a simple spin-coating process.
- Clear 180° ferroelectric phase switching was achieved under ±10 V electrical poling.
- A maximum local piezoelectric response of ~6.65 nm/V was obtained by PFM analysis.
- Depolarized domains exhibited reduced piezo response governed by dipolar relaxation dynamics.
- Nanoscale piezoelectric switching in PVDF parallels bulk shape-memory–induced modulation.

Introduction

Ferroelectric substances are gaining major attention due to their potential applications in nonvolatile random-access memories (NVRAMs), sensors, actuators, transducers, and display panels. Their high memory density, prolonged retention times, and quick read/write speeds are the reasons for this **[1–4]**. Ferroelectric nanostructures have sparked significant theoretical and commercial interest as the demand for miniaturized electronic devices has increased **[5, 6]**. The growing use of a ferroelectric nanostructures in storage systems has resulted in a surge in research into the kinetics of polarization **[7]**. To improve the performance of nanoscale devices, ferroelectric polarization in nanostructures must be precisely controlled **[8, 9]**. The slow loss of polarization brought on by the creation of a depolarized field is a major obstacle to using a ferroelectric capacitor in electrical devices **[10–12].** Many studies concentrated on understanding polarization stability through substrate-induced compressed strain **[13, 14]**, selecting materials for electrodes with a shorter screening length **[15,16]** and using initial-principles calculations to design interfaces **[17–19]**.

Early ferroelectric non-volatile storage investigation made use of small films of a ferroelectric perovskite oxide, which have bistable polarization states (0 and 1) at zero bias **[20–22]**. Ferroelectric memory devices are categorized as either destructive or non-destructive. Destructive devices, such as ferroelectric capacitor-based memory elements, switch between polarization states to store data. However, reading data in the destructive mode erases one polarization state, necessitating a rewriting cycle. This process increases access time, requires a larger memory cell area for additional circuitry, and shortens operational life **[23–26].** Another class of responsive materials are shape memory polymers (SMPs) that distinguish themselves by their ability to be deformed to a temporary shape that is fixed until a suitable trigger (e.g., temperature, light, pH) is added to initiate the recovery process back to their original, permanent shape. Current research is striving for designs of new SMPs that change more than just their shape upon triggering **[27]**.

In particular, most devices are built using Pb-containing compounds like PZT, owing to their outstanding ferroelectric properties **[28,29].** However, since PZT poses health risks, scientists are trying to substitute it in gadgets with eco-friendly substances that have identical or better ferro and their piezoelectric attributes. Most studies show that domain retention behavior is significantly influenced by making voltage width and height, domain size, film depth, strain within the film, atmosphere humidity, and temperature, as well as other factors. Among organic materials, PVDF has shown great promise because of its flexible piezoelectric coefficient, superior thermal stability, and no toxicity **[30,31].** There are five semi crystalline polymorphs of PVDF: α, β, γ, δ, and ε. The most often studied and utilized are α, β, and γ. After cooling from the melt, the most stable and common form is the α-phase, so it exhibits a semi-helical their structure. However, it is non-polar and lacks electroactive properties. The polar β, γ, and δ phases have aligned molecular dipoles, created a net dipole moment and allowed for electroactive behavior **[32–33]**.

So far, only limited efforts have been devoted to investigating nanoscale ferroelectric domain relaxation in PVDF bulk materials and thin films **[30]**. Ferroelectric switching mechanisms in PVDF are strongly influenced by molecular dipole orientation, polymer confinement, and structural imperfections associated with its crystalline phases. To probe trapped polarization energy and ferroelectric domain–based information storage in PVDF thin films, piezo response force microscopy (PFM) was employed owing to its high lateral resolution, nondestructive nature, and ability to locally manipulate polarization states. To the best of our knowledge, solvent-dependent ferroelectric domain relaxation in lead-free PVDF thin films has not yet been reported. The choice of solvent plays a critical role in determining crystalline phase formation and dipole mobility, thereby directly affecting polarization stability and relaxation times. In particular, DMF-induced crystallization can promote electroactive β-phase formation, analogous to mechanically driven crystal phase transitions observed in shape-memory PVDF systems, where reversible deformation modulates piezoelectric response. In this work, we investigate surface screening energy dynamics in interconnected PVDF nanodots and their dependence on nanoscale ferroelectric switching and relaxation behavior using real-time PFM. Furthermore, the relaxation kinetics are quantitatively analyzed using an exponential time-dependent model to elucidate the underlying dipole relaxation mechanisms.

Experimental part

The PVDF powder (Sigma-Aldrich) dissolved in Dimethylformamide (DMF) and stirred at 60°C for over 60 minutes until transparent, yielding a 5ml solution was made by dissolving 2 wt.% PVDF solution (molecular weight 534,000 g/mol) and a density of 1.74 grams per milliliter in type of powder (purity of 99.99%; Sigma Aldrich), in DMF solvent. Moreover, the solution was coated to a specifically on Polar Industrial Cooperation-1 (PIC-1) micro slides from the Blue Star brand, with dimensions of 1 x 1 cm^2, PVDF thin film thickness 218nm. To create PVDF interconnected nanodots, the solution was dropped onto an in-situ annealed glass substrate (130°C) and spun for one minute at 6000 rpm with a homemade spin coater. During deposition and annealing, the distance between the substrate and the halogen lamp was kept constant at 5 cm. The spin coater, built around a DC motor, was controlled by a 555 timer with pulse-width modulation. This process was carried out under a unique Still & Hot (SH) atmosphere, where deposition occurred on a heated substrate **[30].** Its surface morphology, height, roughness, ferroelectric and piezoelectric characteristics, and local relaxation kinetics were investigated using Piezo force mode of Bruker MM8 scanning force microscopy. The ferroelectric domains underwent 180° phase reversal when different DC voltages (±10 V_{dc}) biased and alternating current (AC) amplitudes (2 kHz) were applied to visualize the interconnected nanodots responses.

Result and Discussion

According to initially reports, the films showed that the peaks at 824 cm^{-1} and 1176 cm^{-1} their corresponding β and γ phases cm^{-1} in FTIR-ATR measurements indicated that the film showed a polar phase **[30]**. This method measures the mechanical vibrations of a conductive AFM tip that comes into contact with the sample. Applying a low amplitude alternating electric potential between the tip and the bottom electrode causes the sample to periodically deform via the converse piezoelectric effect. Fig.1 shows PFM scanned height and phase images of 6 × 6 μm^2 without polling. Within 6 x 6 μm^2, 3 × 3 μm^2 were selected and poled at -10Vdc, within 3 × 3 μm^2 were selected 1 ×1 μm^2 and poled at +10 $V_{dc,}$ and after poled, the same 6 × 6 μm^2 area was scanned again. The observation of heights images Fig. 1(a_1 & a_4) reveals that the entire region 6 × 6 μm^2 no leakage current and damage after poled ±10 V_{dc} Sample response after applied 10V_{ac} as shown Fig.1(b_1& b_2) indicates the expansion of polymer interconnected nanodots in the application -10 V_{dc}, UP polarization has been clearly seen. DOWN polarization has been shown in Fig.1(b_3), in that image the interconnected nanodots were strained towards glass substrate. Overall polarization of both ±10 V_{dc} was scanned by 10 V_{ac} as shown in Fig.1 (b_4), which shows both white and dark contrast as UP and DOWN polarization. These results proved the interconnected nanodots has reversible polarization and exhibits ferroelectric nature which was proved by piezo response hysteresis loop (Phase vs DC Bias). The butterfly curve (Amplitude vs. DC Bias) was used to study the piezoelectric coefficient (d_{33}) of 6.3 nm/V of out-of-plane direction Fig.2. The intrinsic polarity

of the interconnected nanodots in the PVDF thin film gets the UP-polarization state to be dominant. The time-lapse pictures of the UP and DOWN polarized domains in the poled regions of the film, taken at 2 kHz with a 10 V_{ac} voltage, are shown in Fig.1 **[34]**. Self-polarized regions are possible at ferroelectric electrode interfaces **[35, 36]**.

As illustrated in Fig.3 the motion of the tip is tracked at various points after polling in order to measure the amplitude and phase of the mechanical vibration and produce images that reveal the direction of the local polarization. The bright UP polarized state is able to overcome the screening molecule energy at the boundary because of the influence of electrode interface effects on the DOWN (DARK) polarized state. Fig.3(a_1, a_2, a_3, & a_4) PFM phase images demonstrate, over a few hours, the DARK areas progressively change into BRIGHT areas. This change may be due to a spontaneous reorientation of the polarization direction caused by the strain gradient at the domain boundary molecules **[37-40]**, which have been clearly seen in Fig.3(b_1, b_2, b_3 & b_4) amplitude images. Nanoscale switching measurements were used to investigate the switching kinetics **[41-45].**

Reversible kinetics of 6000 rpm PVDF film

The image in Fig. 3 PFM depicts a dynamic study of polarization changes over time, particularly in bright and dark regions. The distinct PFM images Fig. 4 (a_1), (a_2), (a_3) & (a_4) and labels (d_1), ($d_{2)}$, ($d_{3)}$, (d_4), and (s_1) most likely correspond to different spatial points or regions within the analyzed sample.
Fig.4 (a_1), at t_1 = 0.00 hr indicated the beginning state of polarized states, in that states there was no changes in the states of polarizations. This frame depicts the initial polarization state, probably under unified terms. The analysis appears to be focused on a central feature the red marked region.

In down polarization, dark regions correspond to bright regions in up polarization Fig.4(a_1). In Fig.4 (a_2), (t_2) = 1.00 hr that means after one hour the DOWN polarized state of domains present in the corners of the dark regions were switching towards BRIGHT regions of up polarized states of domains as mentioned as (d_1), (d_2) & (d_3). After 2 hours, a similar process occurs, but the left corner (d_1 & d_4) and the right corner (d_2 & d_3) differ notably at Fig.4 (a_3). By 2.40 hours, as depicted in Fig. 4(a_4), more parts of the down polarization have completely transformed, with high levels of up polarization dominating the structure but till some molecular chains were not oriented UP direction as mentioned as red circle (S_1). The (d_1), (d_2), (d_3) & (d_4) domains penetration from DOWN polarized state into UP polarized state were completed at 2.00 hr but S_1 domains of DOWN polarized state remains up to 2.40 hr as shown in the Fig.5-time V_s penetration length.

Application

To understand the piezo and ferroelectric nature of depolarized domains from DARK to BRIGHT after poling +10V (Yellow circle in Fig.6(a_2), partially depolarized domain (Rose circle in Fig.6(a_2), and not depolarized domain (White circle in Fig.6(a_2), selected respective three domains and applied ±10 V by utilizing ramp technique as shown in Fig.6. In Fig.6(a_1) indicated that phase image at T=2.00 hr, in that 1

x 1 μm^2 poled +10 V dc after poling (white square box) as shown in Fig.6(a_2). The depolarized domain from DARK to BRIGHT showed symmetric ferroelectric and piezoelectric coefficient d_{33}=3.85 nm/V as shown Fig.6(a_3). The partially depolarized domain from DARK to BRIGHT showed non symmetric ferroelectric due to piezoelectric coefficient d_{33}=4.55 nm/V as shown Fig.6 (a_4). The not depolarized domain showed symmetric ferroelectric and piezoelectric coefficient d_{33}=4.00 nm/V as shown Fig. 6 (a_5). All of the steps displayed that the bright UP polarization state influence the DOWN (DARK) polarized state to get around the screening molecule energy at the boundary because of the results of the interface of the electrodes. One possible explanation for the polarization directions spontaneous orientation is the strain gradient at the domain's boundary molecules. The best fit was given by the stretched exponential function model f=1-e-k(t-t_0) n, as shown in Fig. (7) k, n, and to (time taken to start the reversible polarization) are the critical parameters in this model, where "f" stands for the size of the segment in the reversed domains **[30, 46]**. The Fig .1 displays a series of AFM images captured at various time intervals during a rotation process. The first image was taken before rotation, and the subsequent images show how the surface changed after 41, 52, and 60 minutes of rotation.

The switchable piezoelectric behavior observed in shape-memory-programmed PVDF systems is fundamentally governed by the evolution of electroactive β-phase crystals and their associated dipole alignment. In CP1 samples, the piezoelectric coefficient (d_{33}) exhibited a periodic variation during different shape memory stages, reaching a maximum value of ∼9 pC/N in the fixation state due to enhanced β-phase formation induced by mechanical stretching, while significantly lower values were observed in the original and recovery states **[47]**. A similar mechanism operates at the nanoscale in interconnected PVDF nanodot films, where electrical poling induces reversible polarization switching confirmed by 180° phase contrast in PFM measurements. The maximum local piezoelectric response (d_{33} ≈ 6.65 nm/V) arises from efficient dipole alignment within highly ordered nanodots, whereas partially and fully depolarized domains exhibit reduced responses due to dipolar relaxation. The stretched-exponential relaxation behavior further highlights the intrinsic stability and time-dependent evolution of polarization states. Collectively, these results demonstrate that both mechanically and electrically induced switchable piezoelectricity in PVDF originate from controllable crystal phase transitions and dipole dynamics, spanning from bulk shape-memory systems to nanoscale ferroelectric architectures.

The graph compares experimental data with a stretched exponential function fit to show the fraction of reversed domains over time. The fraction of reversed domains is displayed on the y-axis, varying from 0 to 1, while the x-axis shows time in minutes, from 0 to 200. This behavior is simulated using a stretched exponential in nature activity, represented by a red dashed a line. To simulate this behavior, a stretched exponential function is utilized, which is symbolized by the red dashed line. This function includes two parameters, k and n. The graph focuses on values for k = 2.48 x $10^{-6}$and n = 2.5. The strain gradient at the domain boundary molecules may be the cause of the polarization direction's spontaneous orientation. f=1-e-k(t-t_0) n, the model of the stretched exponentially activity, gave the best fit, as shown in Fig. (7) Critical parameters in this model are k, n, and to (time taken to start the reversible polarization), where f stands for the area fraction of the reversed domains.

Conclusion

The study of interconnected PVDF nanodots formed by spin coating at 6000 rpm revealed excellent ferroelectric and piezoelectric properties, before polling, after polling, depolarized domains and partially depolarized domains as confirmed by piezo force microscopy. A distinct 180º phase reversal was observed in poling experiments at -10 V (UP polarization) and + 10 V (DOWN polarization), suggesting robust polarization behavior. Interestingly, the domain reversal kinetics demonstrated a natural tendency toward UP polarization in individual nanodots when switched to the DOWN state. Depolarized domains hysteresis and butterfly curves illustrated that molecular chain alien their original position after reversal. Partially depolarized domains asymmetric hysteresis and butterfly curves illustrated that molecular chains were not alien their original position after reversal. A stretched exponential model utilized to accurately describe the relaxation kinetics, emphasizing time-dependent domain dynamics. These findings indicate the 6000 rpm PVDF films potential for advanced applications in ferroelectric shape memory systems and flexible electronic devices, owing to their superior structural and functional characteristics.

Declarations

Declaration of Competing Interest:

The authors declare that they have no known competing financial interests or personal relationships that could have appeared to influence the work reported in this paper.

Ethics approval and consent to participate:

Not applicable. This study did not involve human participants or animals.

Consent for Publication:

Not applicable. The authors consent to the publication of this manuscript.

Data availability statement:

If a reasonable request is made, the data will be provided.

Authors Contribution:

First Author: **Shalini Selvam**[1] – Writing – original draft, Methodology, Data curation, Conceptualization-sshalini10072001@gmail.com

Second Author: Suganthi Muthusamy[2] Formal analysis and Editing.

Third Author: M Perumal[3] Formal analysis and Editing.

Fourth Author: Suvitha A[4] Formal analysis and Editing

Fifth Author & Corresponding Author: **M S Ravisankar**[5*] Writing – review & editing, Supervision. ravisankarms775@gmail.com

Sixth Author& Corresponding Author: **V. Balasubramani** [6*] Writing – review & editing, Supervision. balsubramaniv3@gmail.com

Seven Author**:** J. Venkatamuthukumar[7] - Formal analysis and editing- venkatamuthukumar.j@rajalakshmi.edu.in

Acknowledgement:

We sincerely acknowledge UGC, DAE-BRNS, DST, and UGC-SAP for their support. We also extend our gratitude to the Central Instrumentation Facility (CIF) at Pondicherry University for providing necessary resources and facilities.

References

1. Jung, J.; Lee, W.; Kang, W.; Shin, E.; Ryu, J.; Choi, H. Review of Piezoelectric Micromachined Ultrasonic Transducers and Their Applications. J. Micromech. Microeng. 2017, 27, 113001.
2. Wang, Y.; Chen, W.; Wang, B.; Zheng, Y. Ultrathin Ferroelectric Films: Growth, Characterization, and Applications. Materials 2014, 7, 6377–6485.
3. Gao, W.; Zhu, Y.; Wang, Y.; Yuan, G.; Liu, J.-M. A Review of Flexible Perovskite Oxide Ferroelectric Films and Their Application. J. Materiomics 2020, 6, 1–16.
4. Sappati, K. K.; Bhadra, S. Piezoelectric Polymer and Paper Substrates: A Review. Sensors 2018, 18, 3605
5. Ren, Xintong, et al. "Giant energy storage density in PVDF with internal stress engineered polar nanostructures." Nano Energy 72 (2020): 104662.
6. Abel, Stefan, et al. "Large Pockels effect in micro-and nanostructured barium titanate integrated on silicon." Nature materials 18.1 (2019): 42-47.
7. Sun, Haoying, et al. "Nonvolatile ferroelectric domain wall memory integrated on silicon." Nature communications 13.1 (2022): 4332.
8. Gupta, Shashikant, et al. "Multifunctional and flexible polymeric nanocomposite films with improved ferroelectric and piezoelectric properties for energy generation devices." ACS Applied Energy Materials 2.9 (2019): 6364-6374.
9. Chen, Haoyun, et al. "Large electrostrain induced by reversible domain switching in ordered ferroelectric nanostructures with optimized geometric configurations." Nanotechnology 31.33 (2020): 335714.

10. Dawber, M., et al. "Depolarization corrections to the coercive field in thin-film ferroelectrics." Journal of Physics: Condensed Matter 15.24 (2003): L393.
11. Kim, D. J., et al. "Polarization Relaxation Induced by a Depolarization Field<? format?> in Ultrathin Ferroelectric BaTiO 3 Capacitors." Physical review letters 95.23 (2005): 237602.
12. Naveen, C., and M. Muthuvinayagam. "Studies on electrical properties of Chitosan-PVA based biopolymer electrolytes for electrochemical devices." Journal of Polymer Research 30.9 (2023): 353.
13. Ederer, Claude, and Nicola A. Spaldin. "Effect of epitaxial strain on the spontaneous polarization of thin film ferroelectrics." Physical review letters 95.25 (2005): 257601.
14. Choi, Kyoung Jin, et al. "Enhancement of ferroelectricity in strained BaTiO3 thin films." Science 306.5698 (2004): 1005-1009.
15. Choi, W. S., et al. "Dielectric constants of Ir, Ru, Pt, and IrO 2: Contributions from bound charges." Physical Review B—Condensed Matter and Materials Physics 74.20 (2006): 205117.
16. Lu, H., et al. "Enhancement of ferroelectric polarization stability by interface engineering." (2012).
17. Plonka, R., et al. "Impact of the top-electrode material on the permittivity of single-crystalline Ba0. 7Sr0. 3TiO3 thin films." Applied Physics Letters 86.20 (2005).
18. Liu, Xiaohui, et al. "Interface dipole effect on thin film ferroelectric stability: First-principles and phenomenological modeling." Physical Review B—Condensed Matter and Materials Physics 85.12 (2012): 125407.
19. Zembilgotov, A. G., et al. "Ultrathin epitaxial ferroelectric films grown on compressive substrates: Competition between the surface and strain effects." Journal of applied physics 91.4 (2002): 2247-2254.
20. Setter, N., et al. "Ferroelectric thin films: Review of materials, properties, and applications." Journal of applied physics 100.5 (2006).
21. Ducharme, Stephen, et al. "Ferroelectric polymer Langmuir-Blodgett films for nonvolatile memory applications." IEEE Transactions on Device and Materials Reliability 5.4 (2005): 720-735.
22. Park, Youn Jung, et al. "Control of thin ferroelectric polymer films for non-volatile memory applications." IEEE Transactions on Dielectrics and Electrical Insulation 17.4 (2010): 1135-1163.
23. Sheikholeslami, Ali, and P. Glenn Gulak. "A survey of circuit innovations in ferroelectric random-access memories." Proceedings of the IEEE 88.5 (2000): 667-689.
24. Bagla, Anshika, et al. "ZnO@ C/PVDF Electrospun Membrane as a Piezoelectric Nanogenerator for Wearable Applications." The Journal of Physical Chemistry C (2025).
25. Parangusan, Kiruthika, et al. "Biocompatible neem gum-modified polyvinyl alcohol composite as dielectric material for flexible energy devices." Heliyon 10.7 (2024).
26. Ishiwara, Hiroshi, et al. "Ferroelectric-gate field effect transistor memories." (2016): 141-155.
27. Hoeher, Robin, et al. "Shape-Memory PVDF Exhibiting Switchable Piezoelectricity." Macromolecular Rapid Communications 36.23 (2015): 2042-2046.

28. Setter, N.; Damjanovic, D.; Eng, L.; Fox, G.; Gevorgian, S.; Hong, S.; Kingon, A.; Kohlstedt, H.; Park, N. Y.; Stephenson, G. B.; Stolitchnov, I.; Taganstev, A. K.; Taylor, D. V.; Yamada, T.; Streiffer, S. Ferroelectric Thin films: Review of Materials, Properties, and Applications. J. Appl. Phys. 2006, 100, 051606.
29. Safaei, M.; Sodano, H. A.; Anton, S. R. A Review of Energy Harvesting Using Piezoelectric Materials: State-of-the-Art a Decade Later (2008–2018). Smart Mater. Struct. 2019, 28, 113001
30. Yin, Jia-Yi, et al. "Effects of solvent and electrospinning parameters on the morphology and piezoelectric properties of PVDF nanofibrous membrane." Nanomaterials 12.6 (2022): 962.
31. Filip, Petr, Jana Zelenkova, and Petra Peer. "Electrospinning of a copolymer PVDF-co-HFP solved in DMF/acetone: Explicit relations among viscosity, polymer concentration, DMF/acetone ratio and mean nanofiber diameter." Polymers 13.19 (2021): 3418.
32. Kabir, Ekramul, et al. "Pure β-phase formation in polyvinylidene fluoride (PVDF)-carbon nanotube composites." Journal of Physics D: Applied Physics 50.16 (2017): 163002.
33. Ravisankar, M. S., and R. B. Gangineni. "Study of relaxation kinetics in PVDF interconnected nanodots using piezo force microscopy." Journal of Materials Science: Materials in Electronics 34.8 (2023): 704.
34. Huey, Bryan D., et al. "High speed SPM applied for direct nanoscale mapping of the influence of defects on ferroelectric switching dynamics." Journal of the American Ceramic Society 95.4 (2012): 1147-1162.
35. Güthner, P., and K. Dransfeld. "Local poling of ferroelectric polymers by scanning force microscopy." Applied Physics Letters 61.9 (1992): 1137-1139.
36. Sun, Haoying, et al. "Nonvolatile ferroelectric domain wall memory integrated on silicon." Nature communications 13.1 (2022): 4332.
37. Li, Bo, et al. "Abnormal high voltage resistivity of polyvinylidene fluoride and implications for applications in high energy density film capacitors." Applied Physics Letters 113.19 (2018).
38. Sharma, Pankaj, et al. "High-resolution studies of domain switching behavior in nanostructured ferroelectric polymers." Nano letters 11.5 (2011): 1970-1975.
39. Chen, Xiang-Zhong, et al. "Nano-imprinted ferroelectric polymer nanodot arrays for high density data storage." Advanced Functional Materials 23.24 (2013): 3124-3129.
40. Nakagawa, Yuuta, et al. "Domain switching kinetics in vinylidene fluoride/tetrafluoroethylene copolymer thin films." Japanese Journal of Applied Physics 55.10S (2016): 10TA12.
41. Sharma, Pankaj, et al. "Orientational imaging in polar polymers by piezoresponse force microscopy." Journal of Applied Physics 110.5 (2011).
42. Vizdrik, G., et al. "Kinetics of ferroelectric switching in ultrathin films." Physical Review B 68.9 (2003): 094113.
43. Gaynutdinov, R. V., et al. "Polarization switching kinetics at the nanoscale in ferroelectric copolymer Langmuir–Blodgett films." Applied Physics Letters 92.17 (2008).

44. Konno, Atsushi, et al. "Polarization reversal in ferroelectric fluoro-polymers." Japanese Journal of Applied Physics 39.9S (2000): 5676.
45. Furukawa, Takeo, Takashi Nakajima, and Yoshiyuki Takahashi. "Factors governing ferroelectric switching characteristics of thin VDF/TrFE copolymer films." IEEE Transactions on Dielectrics and Electrical Insulation 13.5 (2006): 1120-1131.
46. Pradhan, Soumen, et al. "Thickness-dependent domain relaxation dynamics study in epitaxial K0. 5Na0. 5NbO3 ferroelectric thin films." ACS Applied Materials & Interfaces 13.30 (2021): 36407-36415.
47. Tu, Youlei, et al. "Switchable piezoelectricity of Polyvinylidene fluoride films induced by crystal transition in shape memory process." ACS Applied Materials & Interfaces 14.35 (2022): 40331-40343.

Figures

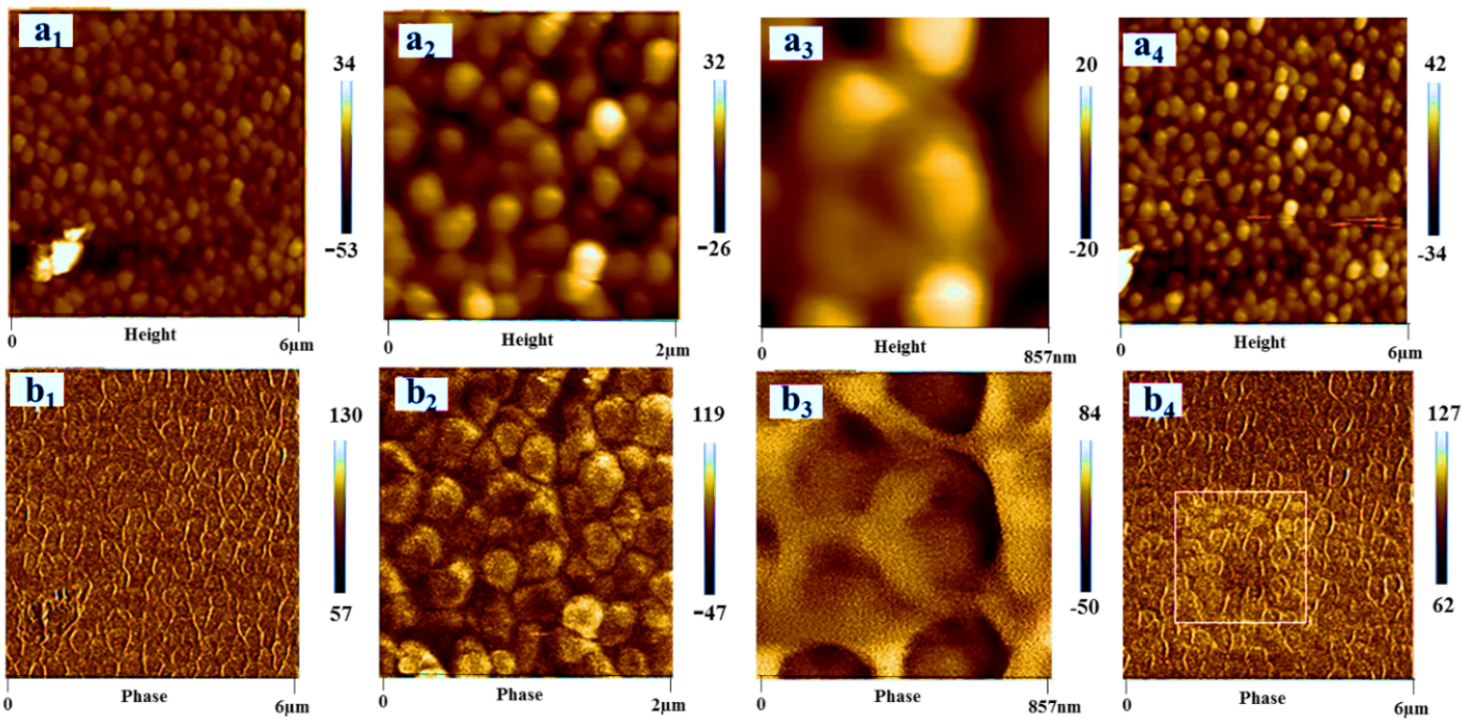


Figure 1

(a_1). PFM height image before polling, (a_2) Height image of -10 V poled area (a_3) Height image of +10 V poled area and (a_4) Height image of after poled (b_1), (b_2), (b_3) and (b_4) PFM Phase images before polling -10 V poled, + 10 V poled and after poled respectively on interconnected PVDF nanodots.

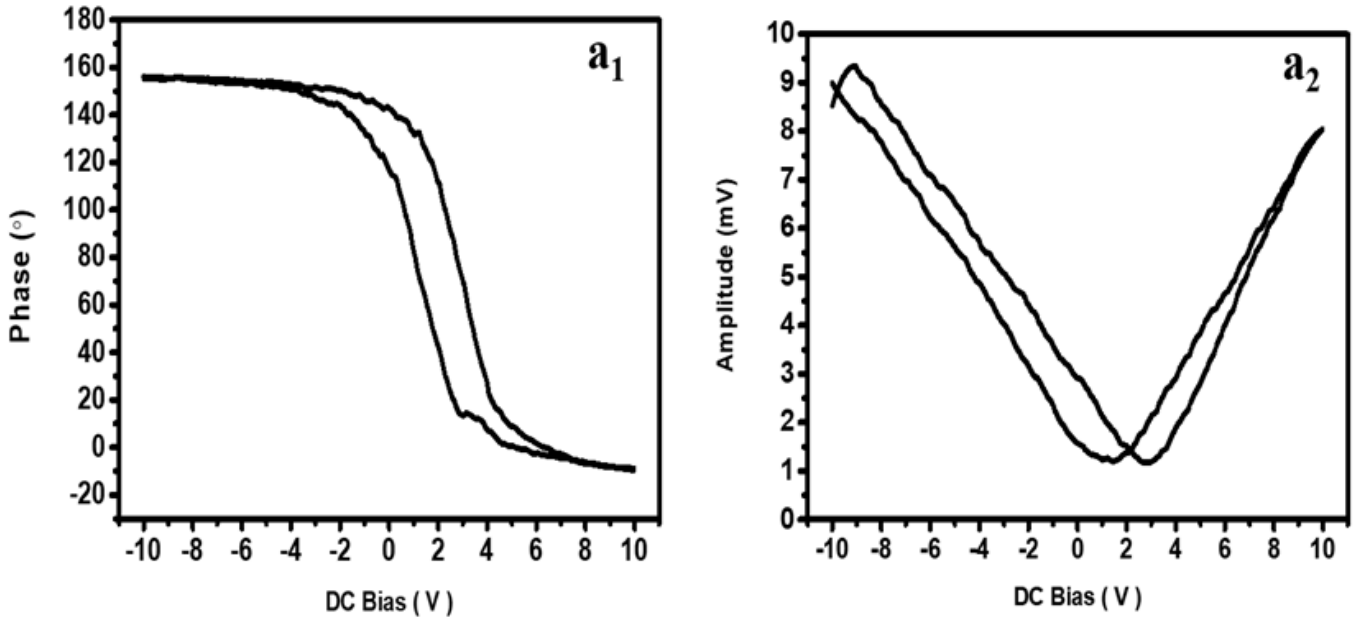


Figure 2

(a_1) The Hysteresis and (a_2) Butter fly curves.

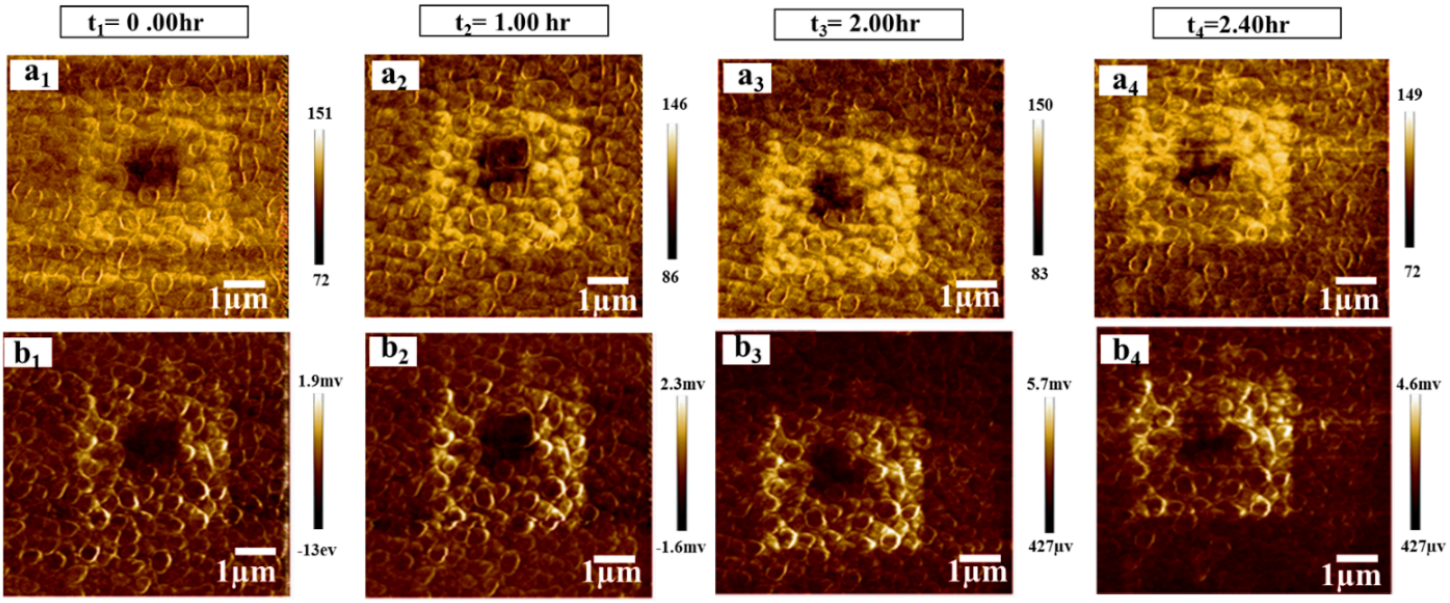


Figure 3

(a_1), (a_2), (a_3) and (a_4) PFM phase images and (b_1), (b_2), (b_3) and (b_4) amplitude images of relaxation kinetics of interconnected PVDF nanodots taken over time.

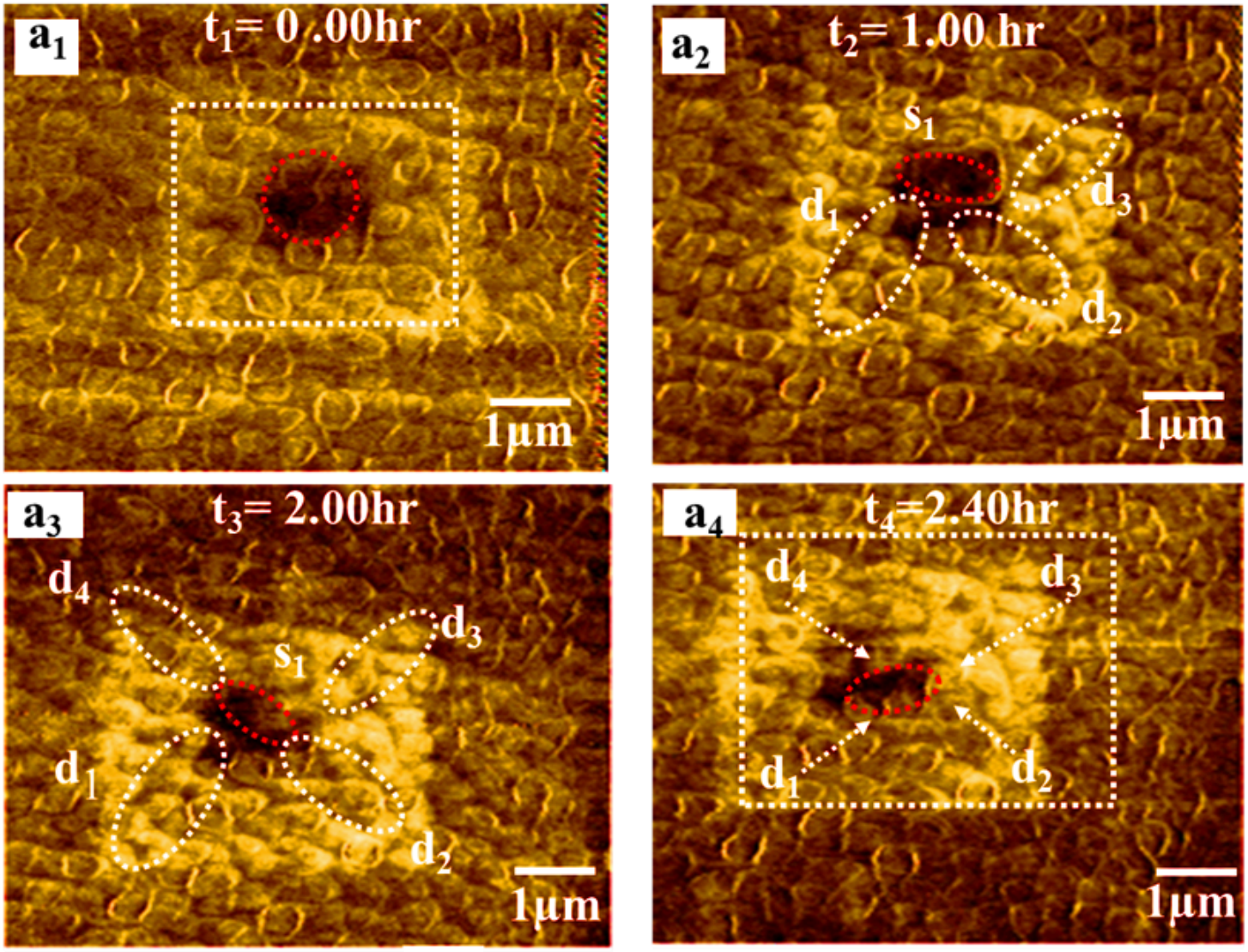


Figure 4

(a_1), (a_2), (a_3) and (a_4) are time-lapsed PFM phase images show domain kinetics at (t_1), (t_2), (t_3), and (t_4) for 2.40 hr of interconnected PVDF nanodots.

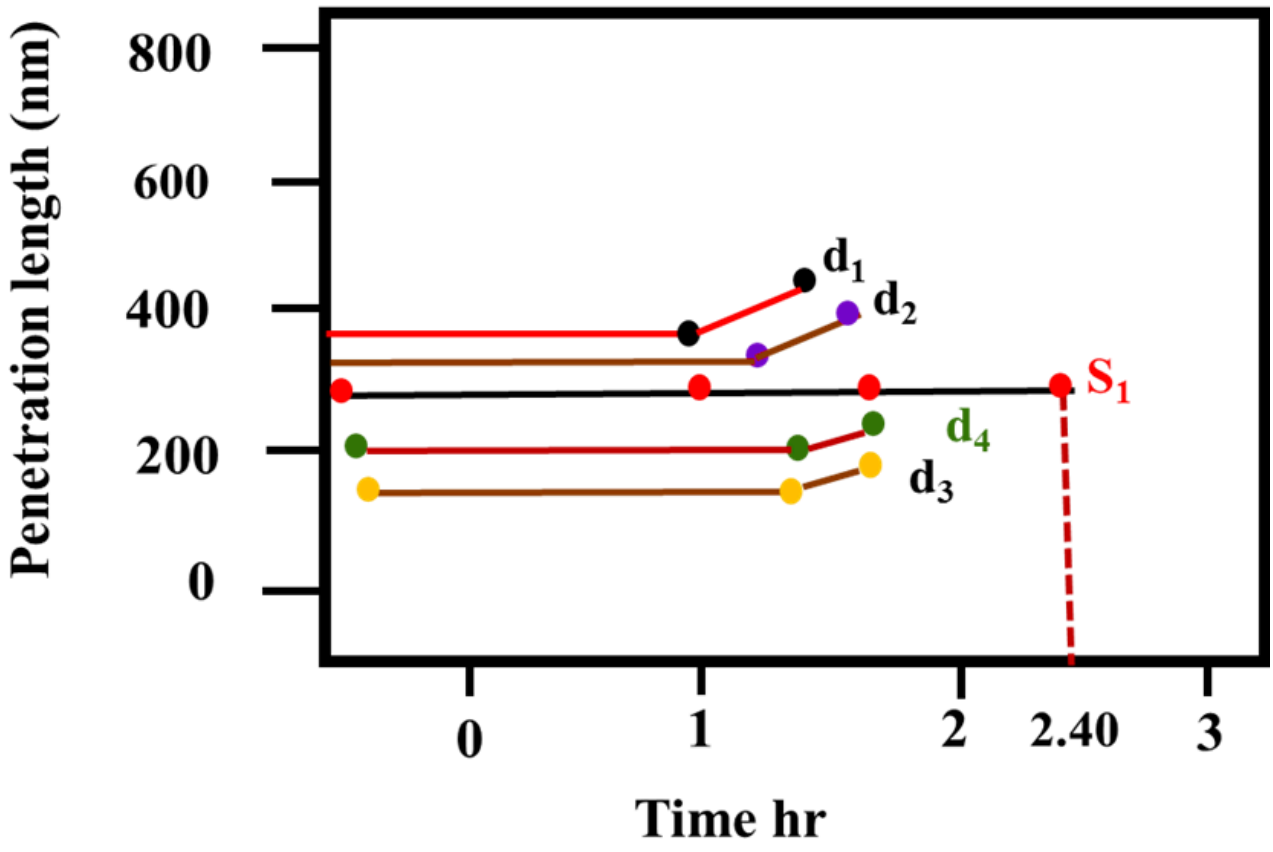


Figure 5

Penetration length of domains derived as a function of time of interconnected nanodots.

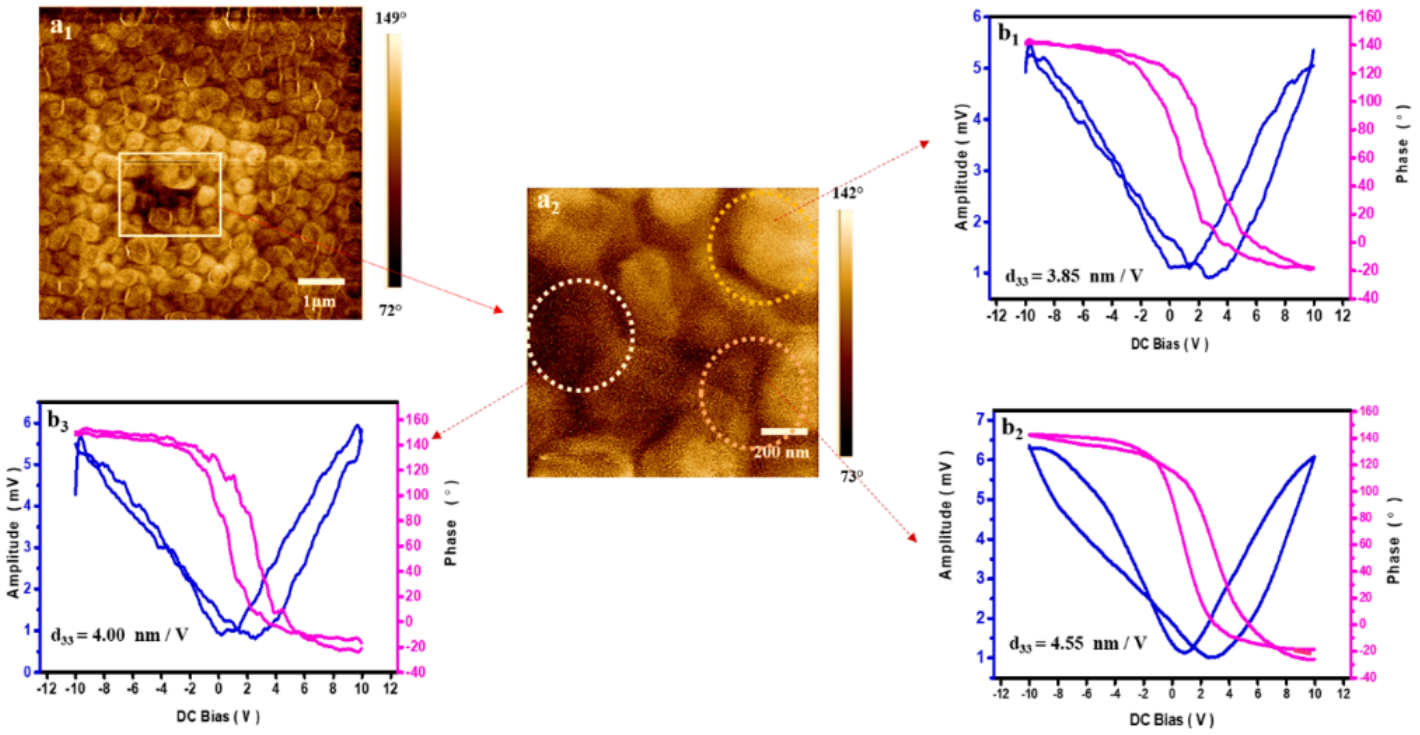


Figure 6

(a_1) PFM phase image at T=2.00 hr (a_2) Phase image of 1 x 1 μm^2 poled +10 V dc after penetration of UP polarization, (b_1) Hysteresis and Butter fly curves of depolarization UP domain (b_2) Hysteresis and Butter fly curves of partially depolarization UP domain and (b_3) Hysteresis and Butter fly curves of not depolarization DOWN domain.

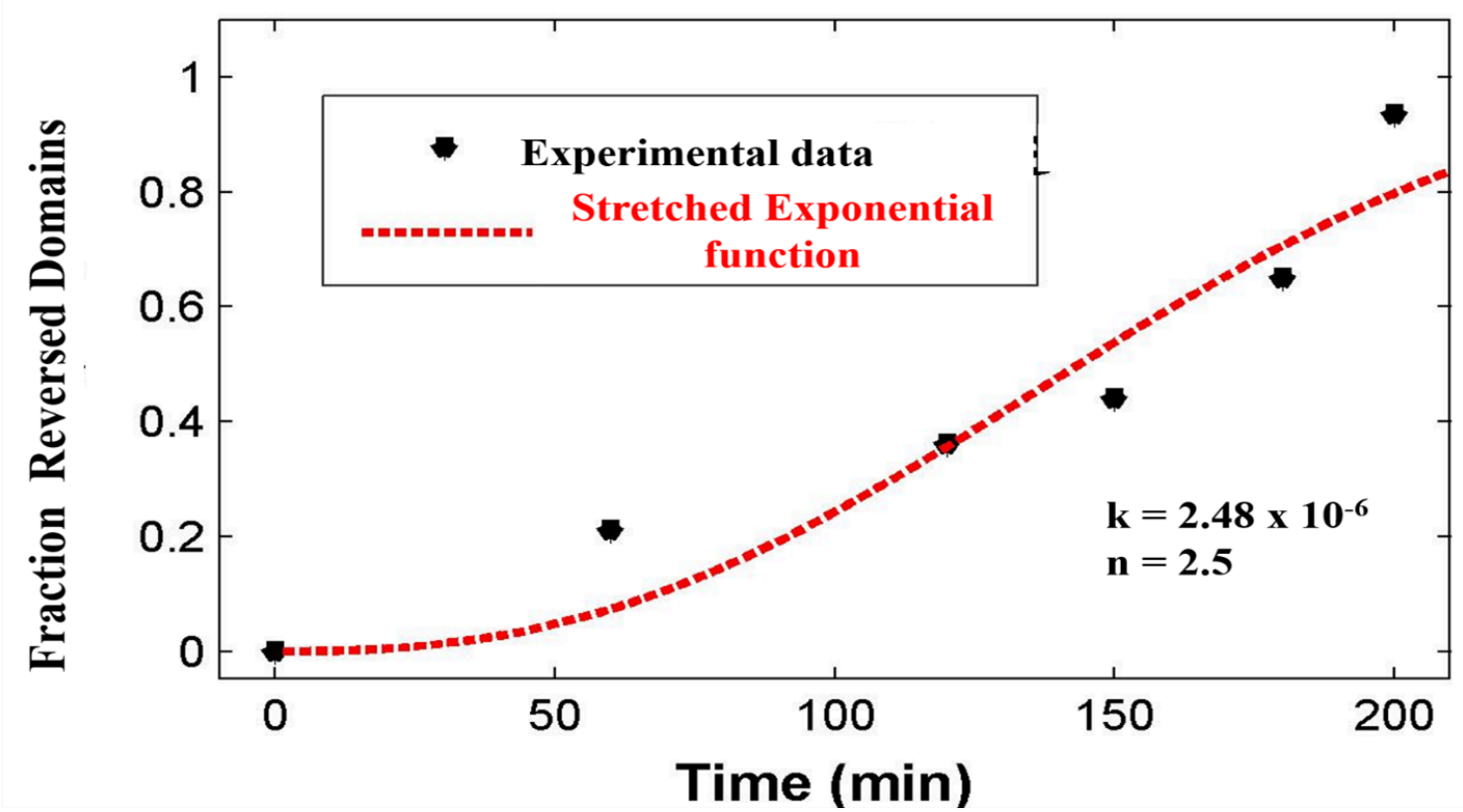


Figure 7

Time-dependent fractional area of inverted domains for downward depolarization from DOWN to UP polarizations fitted to stretched exponential function of interconnected PVDF nanodots.